Inorg. Chem. **2005**, *44*, 7918–7924

Moisture-Triggered 1,3,5-Triazine-Based Cu^{II} Molecular Switch: a Combined X-ray Single-Crystal and Powder Diffraction Study

Hélène Casellas,[†] Patrick Gamez,*[,†] Jan Reedijk,[†] Ilpo Mutikainen,[‡] Urho Turpeinen,[‡] Norberto Masciocchi,*[,§] Simona Galli,[§] and Angelo Sironi[£]

Leiden Institute of Chemistry, Gorlaeus Laboratories, Leiden University, P.O. Box 9502, 2300 RA, Leiden, The Netherlands, Department of Chemistry, Laboratory of Inorganic Chemistry, University of Helsinki, FIN-00014 Helsinki, Finland, Dipartimento di Scienze Chimiche e Ambientali, University of Insubria, via Valleggio 11, I-22100 Como, Italy, and Dipartimento di Chimica Strutturale e Stereochimica Inorganica, University of Milano, via Venezian 21, I-20133 Milano, Italy

Received June 8, 2005

A solvothermal synthetic procedure has been exploited to prepare the new $[Cu_3L(NO_3)_6]_n$ coordination polymer (**1**) by reaction of the polydentate *N,N′*-{2,4-di-[(di-pyridin-2-yl)amine]-1,3,5-triazine}ethylenediamine ligand (opytrizediam L) with copper(II) nitrate. **1** has been structurally characterized by means of the conventional X-ray single-crystal diffraction technique. It crystallizes in the monoclinic *C*2/*c* space group with $a = 16.830(3)$, $b = 20.701(4)$, $c = 18.170(4)$ Å, $\beta = 113.26(3)°$, $V = 5816(2)$ Å^3, $Z = 4$. **1** consists of trinuclear $Cu_3L(NO_3)_5$ units connected by means of a nitrato-O,O′ bridge. The resulting chains are involved in weak interchain head-to-tail π–π stacking interactions. In the presence of moisture, **1** is readily converted into the hydrated $[Cu_3L(NO_3)_5](NO_3)\cdot H_2O$ form (**2**). This second phase, monoclinic $P2_1/c$, consists of isolated $[Cu_3L(NO_3)_5]^+$ and $(NO_3)^-$ ions which accommodate water molecules in the crystal lattice. These subtle chemical and structural modifications accompanying the moisture-triggered **1**-to-**2** transformation have been demonstrated through a X-ray powder diffraction study. A thermodiffractometric analysis has evidenced that this solid-to-solid transformation is fully reversible, i.e., thermally induced dehydration of **2** restores **1**. The analysis of the temperature dependence of the magnetic susceptibility for **2** has revealed very weak ferromagnetic interactions, consistent with the large Cu···Cu separation (ca. 7.5 Å) in the trinuclear units.

Introduction

In recent years, a tremendous effort has been devoted to the rational design of metal coordination complexes with polymeric architectures.[1−6] Rapidly, great advances have been made and a wide array of polymeric networks, and e.g., chains,[7−9] ladders,[10] helices,[11] and honeycombs[12] could be accessed.[5] Several factors are known to influence the architecture of a polymer,[3,11,13−18] notably the ligand nature (connectivity, topology), the counterions, and the reaction

* To whom correspondence should be addressed. E-mail: p.gamez@chem.leidenuniv.nl (P.G.); reedijk@chem.leidenuniv.nl (J.R.); norberto.masciocchi@uninsubria.it (N.M.).
[†] Leiden University.
[‡] University of Helsinki.
[§] University of Insubria.
[£] University of Milano.

(1) Batten, S. R.; Robson, R. *Angew. Chem., Int. Ed.* **1998**, *37*, 1461−1494.
(2) Hagrman, P. J.; Hagrman, D.; Zubieta, J. *Angew. Chem., Int. Ed.* **1999**, *38*, 2639−2684.
(3) Champness, N. R.; Schröder, M. *Curr. Opin. Solid State Mater. Sci.* **1998**, *3*, 419−424.
(4) Blake, A. J.; Champness, N. R.; Hubberstey, P.; Li, W. S.; Withersby, M. A.; Schröder, M. *Coord. Chem.* Rev. **1999**, *183*, 117−138.
(5) Moulton, B.; Zaworotko, M. J. *Chem. Rev.* **2001**, *101*, 1629−1658.
(6) Moulton, B.; Zaworotko, M. J. *Curr. Opin. Solid State Mater. Sci.* **2002**, *6*, 117−123.
(7) Bourne, S. A.; Mondal, A.; Zaworotko, M. J. *Cryst. Eng.* **2001**, *4*, 25−36.
(8) Batsanov, A. S.; Begley, M. J.; Hubberstey, P.; Stroud, J. *J. Chem. Soc., Dalton Trans.* **1996**, 1947−1957.
(9) Kondo, M.; Shimamura, M.; Noro, S.; Yoshitomi, T.; Minakoshi, S.; Kitagawa, S. *Chem. Lett.* **1999**, 285−286.
(10) Carlucci, L.; Ciani, G.; Proserpio, D. M. *J. Chem. Soc., Dalton Trans.* **1999**, 1799−1804.
(11) Kang, Y. J.; Lee, S. S.; Park, K. M.; Lee, S. H.; Kang, S. O.; Ko, J. J. *Inorg. Chem.* **2001**, *40*, 7027−7031.
(12) Choi, H. J.; Suh, M. P. *J. Am. Chem. Soc.* **1998**, *120*, 10622−10628.
(13) Min, K. S.; Suh, M. P. *J. Am. Chem. Soc.* **2000**, *122*, 6834−6840.
(14) Hirsch, K. A.; Wilson, S. R.; Moore, J. S. *Inorg. Chem.* **1997**, *36*, 2960−2968.

10.1021/ic0509231 CCC: $30.25
Published on Web 09/14/2005

Chart 1. *N,N′*-{2,4-Di-[(di-pyridin-2-yl)amine]-1,3,5-triazine}ethylenediamine (Opytrizediam)

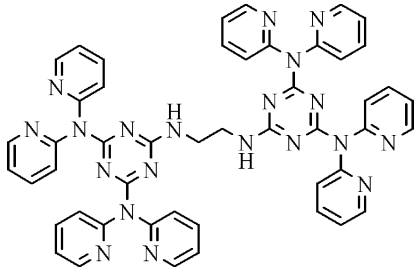

conditions (solvent, temperature, pressure). Along this line, in our group, a great interest is currently focused on the design and the synthesis of rigid and flexible polydentate 1,3,5-triazine-based ligands[19] as building blocks for (supramolecular) polymers.[20,21] It is worth mentioning that the use of a flexible building block with inherent conformational freedom may imply the existence of various supramolecular isomers.[5,22] On the other hand, we are also investigating the influence of the crystallization process conditions on the obtained polymer/complex morphology.[23]

In this study, special attention is given to the flexible polydentate *N,N′*-{2,4-di-[(di-pyridin-2-yl)amine]-1,3,5-triazine}ethylenediamine ligand (opytrizediam L, Chart 1). This ligand is already known for its ability to form polynuclear complexes[24] and even a 1-D polymer[21] upon coordination to Cu^{II} metal centers when the synthesis is performed at room temperature. In this contribution, we focus our investigations on the reaction of this ligand with copper(II) nitrate in acetonitrile at 100 °C under autogenous pressure. The X-ray single-crystal structure of the $[Cu_3L(NO_3)_6]_n$ coordination polymer (**1**) obtained using this solvothermal procedure is here described. Interestingly, it appeared that, in response to moisture, **1** undergoes a rapid chemical and structural transformation in the solid state into the hydrated $Cu_3L(NO_3)_6 \cdot H_2O$ form (**2**). **2** is highly crystalline, and its structure could be retrieved by ab initio X-ray powder diffraction analysis (XRPD). This technique has been recently extensively employed[25] to gather structural information on coordination polymers[26−29] and on their guest-induced transformations.[30−34] The host−guest structure nature of **2**, consisting of an ionic packing of $[Cu_3L(NO_3)_5]^+$ moieties and $(NO_3)^-$ ions hosting clathrated water molecules, has been extracted from XRPD analysis and confirmed by thermogravimetric and differential scanning calorimetric measurements and is presented hereafter. Remarkably, the moisture-induced transformation is fully reversible, as shown by a thermodiffractometric analysis. The temperature-dependent magnetic behavior of the moisture-triggered molecular switch in the phase **2** and its EPR signature are also reported.

Experimental Section

Synthesis of 1. All commercially available reagents were used without further purification. The opytrizediam ligand (L) was prepared according to a reported method.[19] Copper(II) nitrate trihydrate (16 mg, 0.066 mmol) was added to a suspension of opytrizediam (15 mg, 0.016 mmol) in acetonitrile (6 mL). The resulting blue solution was allowed to stand at 100 °C for 12 h under autogenous pressure in a sealed Pyrex tube to form in a good yield $Cu_3L(NO_3)_6$ (**1**) as deep blue needles, which were found to be suitable for X-ray single-crystal diffraction. Since the crystals are extremely sensitive to moisture, they were stored under absolute EtOH, where they are stable, at room temperature, for months. Spectral and analytical data could not be measured, since **1** is extremely sensitive to humidity (even fast transfer to the analytical equipments afforded, in the most fortunate cases, polyphasic mixtures of **1** and **2**), but single-crystal X-ray diffraction under controlled conditions was found to be possible (see below).

Synthesis of 2. 2 is rapidly obtained from **1** as a turquoise-blue powder by exposing **1** for a few minutes in air. Yield (from **1** to **2**): quantitative. Overall yield: 65%. Anal. Calcd for **2**: C, 39.06; H, 2.71; N, 24.68%. Found: C, 39.16; H, 2.83; N, 24.84%. Main IR absorption bands for **2** (cm^{-1}) 3324(w), 1607(m), 1557(m), 1368(s), 1281(s), 1156(m), 1013(m), 804(m), 652(m), 438(m). UV−vis (reflectance, nm) 274, 320 (shoulder), 600−1000 (broad). TG analysis: 1.2% weight loss at 130 °C (1 mol of H_2O per mol trinuclear complex); 43% weight loss at 300 °C [1 mol of H_2O + 8 mol of C_5H_4N (4 mol of dipyridylamine)].

Physical Measurements. Elemental analyses for C, H, and N were performed with a Perkin-Elmer 2400 analyzer. FTIR spectra were recorded with a Perkin-Elmer Paragon 1000 FTIR spectrophotometer, equipped with a Golden Gate ATR device, using the reflectance technique (4000−300 cm^{-1}). Ligand-field spectra were obtained on a Perkin-Elmer Lambda 900 spectrophotometer using the diffuse reflectance technique, with MgO as a reference, over the range 2000−200 nm at room temperature. X-band powder EPR

(15) Withersby, M. A.; Blake, A. J.; Champness, N. R.; Cooke, P. A.; Hubberstey, P.; Li, W. S.; Schroder, M. *Inorg. Chem.* **1999**, *38*, 2259−2266.
(16) Blake, A. J.; Champness, N. R.; Cooke, P. A.; Nicolson, J. E. B.; Wilson, C. *J. Chem. Soc., Dalton Trans.* **2000**, 3811−3819.
(17) Barandika, M. G.; Hernandez-Pino, M. L.; Urtiaga, M. K.; Cortes, R.; Lezama, L.; Arriortua, M. I.; Rojo, T. *J. Chem. Soc., Dalton Trans.* **2000**, *9*, 1469−1473.
(18) Fan, J.; Shu, M. H.; Okamura, T.; Li, Y. Z.; Sun, W. Y.; Tang, W. X.; Ueyama, N. *New J. Chem.* **2003**, *27*, 1307−1309.
(19) de Hoog, P.; Gamez, P.; Driessen, W. L.; Reedijk, J. *Tetrahedron Lett.* **2002**, *43*, 6783−6786.
(20) Gamez, P.; de Hoog, P.; Roubeau, O.; Lutz, M.; Driessen, W. L.; Spek, A. L.; Reedijk, J. *Chem. Commun.* **2002**, 1488−1489.
(21) de Hoog, P.; Gamez, P.; Roubeau, O.; Lutz, M.; Driessen, W. L.; Spek, A. L.; Reedijk, J. *New J. Chem.* **2003**, *27*, 18−21.
(22) Hennigar, T. L.; MacQuarrie, D. C.; Losier, P.; Rogers, R. D.; Zaworotko, M. J. *Angew. Chem., Int. Ed. Engl.* **1997**, *36*, 972−973.
(23) Casellas, H.; Massera, C.; Gamez, P.; Manotti Lanfredi, A. M.; Reedijk, J. *Eur. J. Inorg. Chem.* **2005**, 2902−2908.
(24) de Hoog, P.; Gamez, P.; Luken, M.; Roubeau, O.; Krebs, B.; Reedijk, J. *Inorg. Chim. Acta* **2004**, *357*, 213-218.
(25) Masciocchi, N.; Sironi, A. *C. R. Acad. Sci., Ser. IIc: Chim.* **2005**, in press.
(26) Dikarev, E. V.; Li, B.; Chernyshev, V. V.; Shpanchenko, R. V.; Petrukhina, M. A. *Chem. Commun.* **2005**, *26*, 3274−3276.
(27) Dikarev, E. V.; Shpanchenko, R. V.; Andreini, K. W.; Block, E.; Jin, J.; Petrukhina, M. A. *Inorg. Chem.* **2004**, *43*, 5558−5563.
(28) Dikarev, E. V.; Chernyshev, V. V.; Shpanchenko, R. V.; Filatov, A. S.; Petrukhina, M. A. *Dalton Trans.* **2004**, 4120−4123.
(29) Mascocchi, N.; Ardizzoia, G. A.; Brenna, S.; LaMonica, G.; Maspero, A.; Galli, S.; Sironi, A. *Inorg. Chem.* **2002**, *41*, 6080−6089.
(30) Cingolani, A.; Galli, S.; Masciocchi, N.; Pandolfo, L.; Pettinari, C.; Sironi, A. *J. Am. Chem. Soc.* **2005**, *127*, 6144−6145.
(31) Barea, E.; Navarro, J. A. R.; Salas, J. M.; Masciocchi, N.; Galli, S.; Sironi, A. *J. Am. Chem. Soc.* **2004**, *126*, 3014−3015.
(32) Masciocchi, N.; Galli, S.; Sironi, A.; Barea, E.; Navarro, J. A. R.; Salas, J. M.; Tabares, L. C. *Chem. Mater.* **2003**, *15*, 2153-2160.
(33) Barea, E.; Navarro, J. A. R.; Salas, J. M.; Masciocchi, N.; Galli, S.; Sironi, A. *Inorg. Chem.* **2004**, *43*, 473−481.
(34) Barea, E.; Navarro, J. A. R.; Salas, J. M.; Masciocchi, N.; Galli, S.; Sironi, A. *Polyhedron* **2003**, *22*, 3051−3057.

Table 1. Crystallographic Data and Refinement Details for $[Cu_3L(NO_3)_6]_n$ (**1**) and $[Cu_3L(NO_3)_5](NO_3)\cdot(H_2O)$ (**2**)

	1	**2**
method	SCXRD	XRPD
formula	$C_{48}H_{38}Cu_3N_{26}O_{18}$	$C_{48}H_{40}Cu_3N_{26}O_{19}$
fw (g mol^{-1})	1457.66	1475.67
cryst syst	monoclinic	monoclinic
space group	$C2/c$	$P2_1/c$
a/Å	16.830(3)	16.6345(6)
b/Å	20.701(4)	20.8371(8)
c/Å	18.170(4)	19.1284(9)
β/deg	113.26(3)	116.124(3)
V/Å^3	5816(2)	5952.8(5)
Z	4	4
D_{calc}/g cm^{-3}	1.665	1.646
T/K	173	298
λ/Å	Mo Kα 0.71073	Cu Kα$_1$ 1.5406
μ/mm^{-1}	1.184	20.9
F(000)	2956	2996
reflns collected/unique	20 936/6563 [R_{int} = 0.0531]	n.a.
final R indices [$I > 2\sigma(I)$]	R1 = 0.0443 wR2 = 0.0896	R_{wp} = 0.148 R_p = 0.111
R indices (all data)	R_1 = 0.0921 wR2 = 0.1049	R_{Bragg} = 0.104
GOF	1.019 (on F^2)	3.96 (on y_i)

spectra were recorded on a JEOL RE2x electron spin resonance spectrometer using DPPH (g = 2.0036) as a standard. Magnetic susceptibility measurements were carried out using a Quantum Design MPMS-5 5T SQUID magnetometer at 1000 Oe in the temperature range 5−300 K. Data were corrected for the diamagnetic contributions estimated from the Pascal constants.[35] Thermogravimetric (TG) and differential scanning calorimetric (DSC) analyses were performed on Perkin-Elmer Series 7 equipment, under nitrogen, at a heating rate of 10 °C min^{-1}.

Crystallographic Analysis. Single-Crystal X-Ray Diffraction Analysis for 1. A crystal of **1** was selected for the X-ray measurements and mounted on a glass fiber using the oil drop method,[36] and data were collected at 193 K. The intensity data, collected on a Nonius Kappa CCD diffractometer (graphite-monochromated Mo Kα radiation, ω-2θ scans), were corrected for Lorentz and polarization effects and for absorption. All non-hydrogen atoms were refined anisotropically. The H atoms were introduced in calculated positions and refined with fixed geometry with respect to their carrier atoms. Details of the X-ray single-crystal analysis refinement are listed in Table 1. Crystallographic data for **1** have been deposited with the Cambridge Crystallographic Data Centre as supplementary publication No. CCDC 273557.

X-Ray Powder Diffraction Analysis for 2. Powders of **1**, left in air for a few minutes, rapidly change color, from deep blue to turquoise. This material (**2**) is highly crystalline and was deposited in the hollow of a quartz monocrystal (0.7 mm deep) and measured, in the 5−75° 2θ range, with a Seifert MZVI powder diffractometer equipped with a Ge(111) primary beam monochromator (λ = 1.5406 Å). Its diffraction pattern, although different, showed some similarities with that computed from the single-crystal model derived from **1**. The speed of the solid-to-solid transformation suggested also a structural similarity between **1** and **2**, which was confirmed by autoindexing of the first 30 peaks [TOPAS-SVD:[37] a = 16.64, b = 20.86, c = 19.13 Å, β = 116.1°, M(20) = 23 [37]] and by the subsequent Le Bail fit (cf. Supporting Information) (R_{wp} = 0.061) of the full XRPD pattern with this slightly distorted (and inflated) cell, of slightly lower symmetry ($P2_1/c$, a proper subgroup of $C2/c$, that of **1**). The structural model used for **2** was initially taken from the known coordinates of **1** by allowing a semirigid $[Cu_3L(NO_3)_5]^+$ fragment [flexible at the Cu−ONO$_2$ torsions of the 'external' Cu^{II} ions] and a free nitrate ion to float in the parameter space until a (chemically) satisfactory model (supported by low agreement factors) was found by the simulated annealing technique. Space-filling models and evaluation of the residual cavities clearly indicated the presence of a single crystallographically independent void of ca. 28 Å^3, which was then attributed to the clathrated water molecule evidenced by TG measurements (Figure 1). The final refinement was performed by the Rietveld method using TOPAS-R and the rigid models described above. The fundamental parameter approach, coupled with spherical harmonics description of the peak widths and preferred orientation parameters, was employed. A single isotropic thermal factor was assigned to metal atoms [refined value 5.1(2) Å^2], augmented by 2.0 Å^2 for the lighter atoms. The final Rietveld plot is shown in Figure 2, with the following agreement factors: R_p, R_{wp}, and R_{Bragg} 0.111, 0.148, and 0.104, respectively. The high complexity of the XRPD trace did allow only the refinement of a semirigid fragment from the single-crystal structure of **1**, flexible at Cu−ONO$_2$ torsional angles; the water oxygen atom was kept fixed at the location determined from the analysis of the crystal voids. CCDC reference number CCDC 273556.

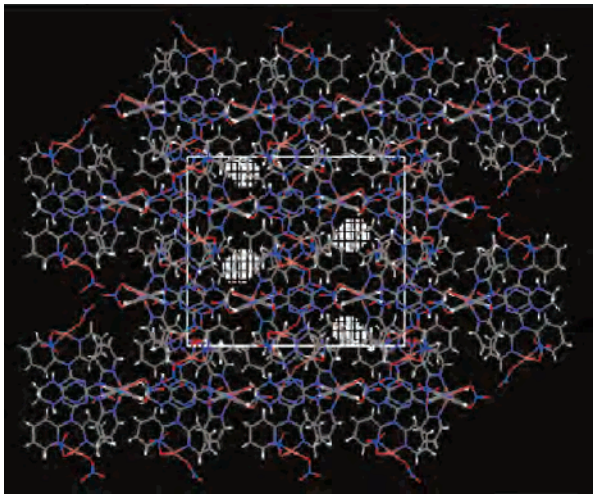

Figure 1. Estimation and localization of the cavities available in **2** for hosting clathrated water molecules, using SMILE;[40] [100] projection, horizontal axis, **b**.

Another series of experiments was performed in order to assess the stability, thermal expansion, and reversibility of the **2**-to-**1** transformation by employing a custom-made heater (supplied by Officina Elettrotecnica di Tenno, Italy) mounted on a Bruker AXS Advance D8 diffractometer: a sequence of scans in the 5−15° 2θ range was performed in the 10−135 °C temperature range (and back), for a total of 26 scans. Relative humidity: 10%. The 3D plot of the raw data is shown in Figure 3, where complete reversibility can be easily appreciated. The Le Bail fit of these diffraction data allowed us to estimate the temperature dependence of the lattice parameters and of the cell volume.

Results and Discussion

Synthesis and Spectroscopy. The solvothermal reaction of the polydentate *N*,*N*′-{2,4-di-[(di-pyridin-2-yl)amine]-1,3,5-triazine}ethylenediamine ligand (opytrizediam L, Chart 1) with Cu^{II} nitrate has afforded a unique moisture-triggered molecular switch. This material, isolated as blue needles in

(35) Kahn, O. *Molecular Magnetism*; VCH Publishers: New York, 1993.
(36) Kottke, T.; Stalke, D. *J. Appl. Crystallogr.* **1993**, *26*, 615−619.
(37) *Topas-R, Bruker AXS: General profile and structure analysis software for powder diffraction data*; Bruker: Madison, WI.

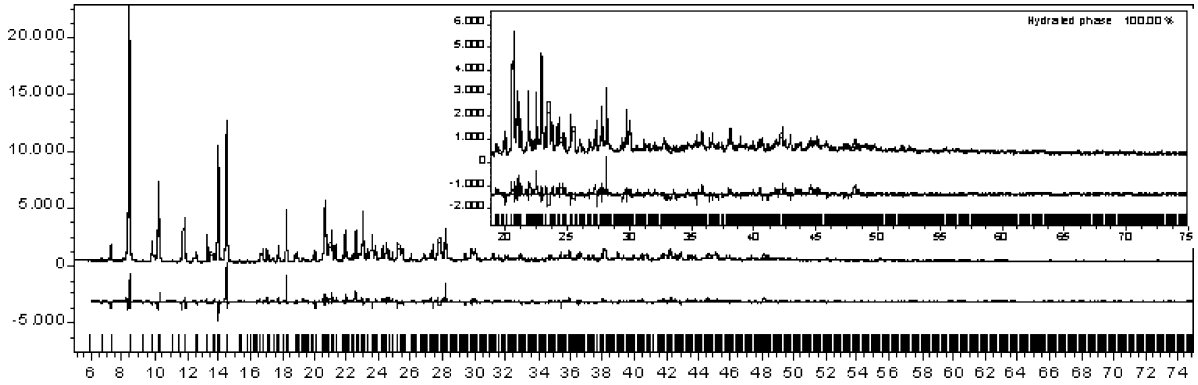

Figure 2. Rietveld refinement plot for **2**, with peak markers and difference plot at the bottom; horizontal scale 2θ, deg; vertical scale, counts. The insert shows the high-angle portion at a 5× magnified scale. The satisfactory, yet imperfect, fit among observed and calculated traces must be attributed to the choice of a (very complex) rigid trinuclear moiety, which was not allowed to fully relax in the simulation of the XRPD pattern of **2**.

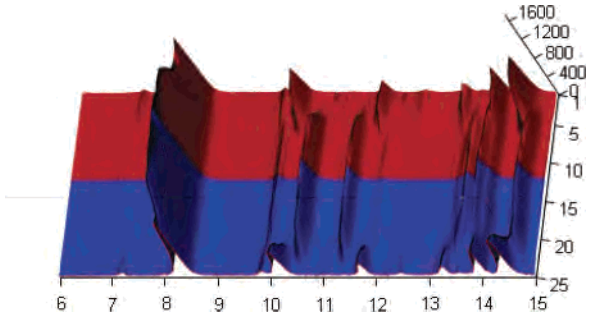

Figure 3. Plot of the XRPD data (26 scans in the 20−135 °C temperature range) during heating (red portion) and subsequent cooling (blue portion). The phase dehydration process can be easily appreciated by the reversible transformation change occurring near 60 °C.

its anhydrous phase, consists of the $[Cu_3L(NO_3)_6]_n$ (**1**) polymer, as evidenced by a conventional X-ray single-crystal diffraction analysis. The hydrated phase of the molecular switch, formulated as $[Cu_3L(NO_3)_5](NO_3)\cdot H_2O$ (**2**), is readily obtained as a turquoise powder suitable for X-ray powder diffraction measurement. Remarkably, thermally induced dehydration (up to 135 °C) of **2** does not involve collapse of the structure, but restores **1** as a blue microcrystalline powder, as confirmed by XRPD.

Due to the high sensitivity of **1** to humidity, spectral and analytical data could be measured only for **2**. The IR spectrum of **2** evidences vibrations at positions in agreement with the coordinated ligand, which can be compared to the vibrations of the free one,[19] especially the band at 1013 cm^{-1}, which is associated with the pyridine ring bending vibration mode, indicates that all the pyridine rings of the opytrizediam ligand are coordinated.[24] In the free ligand, this vibration appears at 995 cm^{-1}. The electronic diffuse reflectance spectrum of **2** presents two main features: a moderate broad band in the 600−1000 nm region and a more-intense absorption band at 274/320 nm. The former signal is assigned to the d−d transition and corresponds to the overlap of absorption bands of tetracoordinated Cu^{II} chromophores in square-planar geometry and of hexacoordinated Cu^{II} ions in distorted octahedral environment. The latter signal is attributed to the ligand to metal charge-transfer transition.

Crystal and Molecular Structure of 1. An ORTEP view of the fundamental repeating unit of the anhydrous form $[Cu_3L(NO_3)_6]_n$ (**1**) is depicted in Figure 4. Selected bond

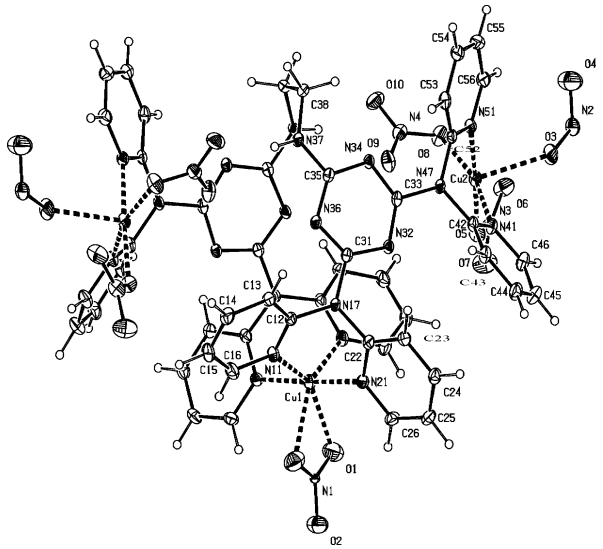

Figure 4. ORTEP view of the fundamental repeating unit of **1**, with a bridging nitrate split on the two 'external' copper sites (displacement ellipsoids drawn at 30%).

Table 2. Selected Bond Lengths (Å) and Angles (deg) for $Cu_3L(NO_3)_6$ (**1**)

Cu1−N11	2.072(3)	Cu2−N51	2.009(3)
Cu1−N21	2.025(3)	Cu2−O3	2.378(2)
Cu1−O1	2.300(3)	Cu2−O5	1.950(2)
Cu2−N41	1.989(3)	Cu2−O8	1.993(2)
N11−Cu1−N11	124.09(15)	O1−Cu1−O1	55.20(15)
N21−Cu1−N21	177.75(15)		

distances and angles are gathered in Table 2. The fundamental repeating unit contains three copper(II) centers, one lying on a crystallographic 2-fold axis (Cu1), the other two (in general position) being crystallographically equivalent (Cu2). Thus, also the opytrizediam ligand displays 2-fold crystallographic symmetry and is bisected at the center of the aliphatic $ArNHCH_2-CH_2NHAr$ bond. Cu1 is in a cis-distorted octahedral environment with a coordination sphere defined by two oxygen atoms of a chelating nitrate ion located at a special position [Cu1−O1 = 2.300(3) Å] and four nitrogen atoms of two didentate dipyridylamine units positioned in general positions [Cu1−N11 = 2.072(3) Å, Cu1−N21 = 2.025(3) Å]. As previously observed, due to the flexibility of the ligand, the two coordinated dipyridylamine units belong to different triazine rings of the opy-

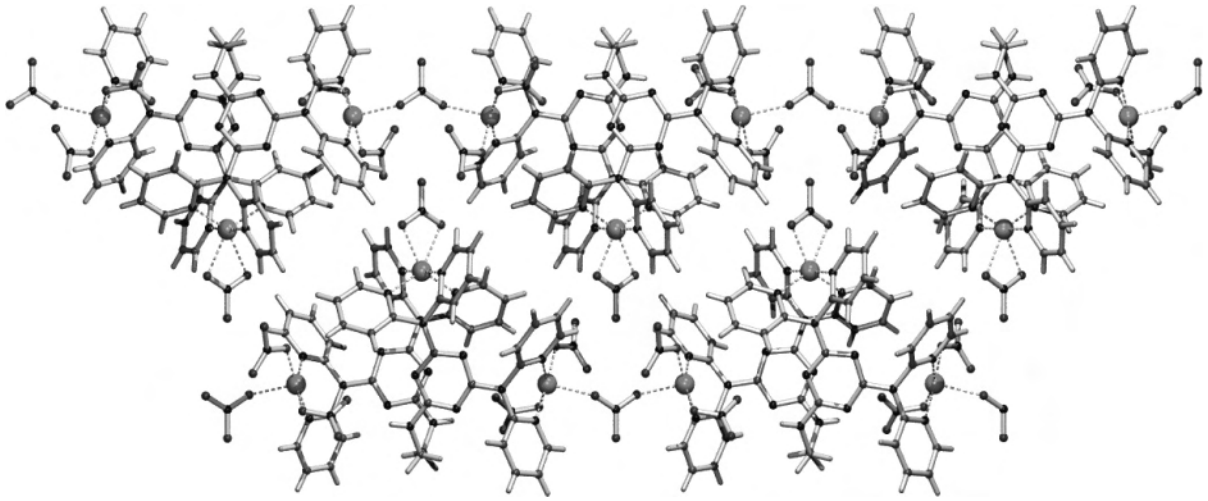

Figure 5. View of the zigzag chain in **1** in the **bc** plane.

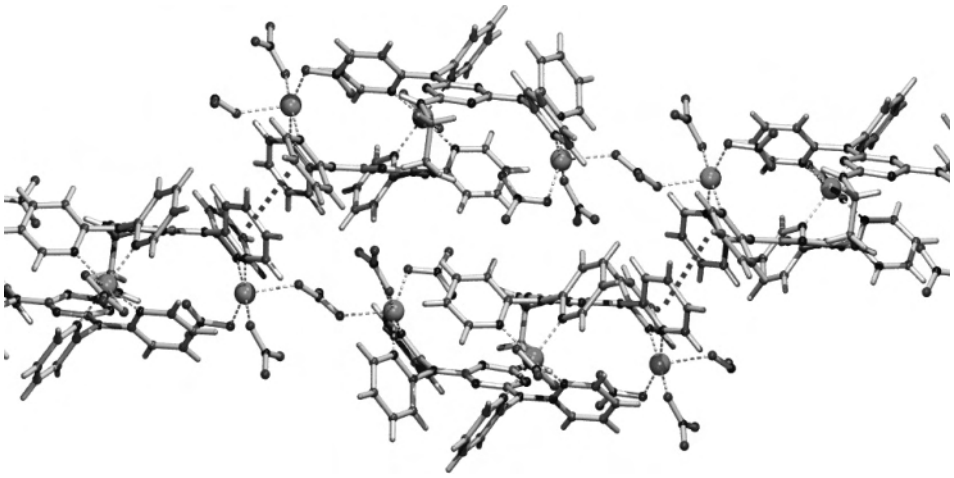

Figure 6. Interchain head-to-tail $\pi-\pi$ stacking interactions in **1**.

trizediam ligand.[21,24] The other two Cu^{II} centers are pentacoordinated in a distorted square pyramidal geometry (τ = 0.21):[39] two nitrogen atoms of a didentate dipyridylamine unit [Cu2−N51 = 2.009(3) Å, Cu2−N41 = 1.989(3) Å], two oxygen atoms of two monodentate nitrate ions [Cu2−O5 = 1.950(2) Å, Cu2−O8 = 1.993(2) Å] define the basal plane, and a weakly coordinated nitrate occupies an axial position [Cu2−O3 2.378(2) Å]. This latter nitrate ion lies on a 2-fold axis and interestingly, acts as a nitrato-O,O′ bridge toward the trinuclear units [Cu2···Cu2 = 6.443 Å]. The so-obtained infinite zigzag self-assembled chain runs along the **c** direction. Figure 5 shows that, in the **bc** plane, the V-shaped trinuclear units of a chain are interdigitated with the trinuclear units belonging to a neighboring one. Noteworthy, when the crystallization reaction between opytrizediam and $Cu(NO_3)_2$ was performed at room temperature, a similar compound was obtained in which, however, the nitrato-O,O′ bridge connects only two trinuclear species into an *isolated* hexanuclear complex.[24] This clearly illustrates, as already recently highlighted,[23] the importance of a solvothermal procedure for preparing polymer-like materials with relevant topology. The 1-D zigzag chains pack together through weak head-to-tail $\pi-\pi$ interactions between pyridine rings, as shown in Figure 6 (3.8−3.9 Å), giving rise to supramolecular sheets in the **ac** plane. No evident interactions, apart from weak van der Waals contacts among the different 'sheets', are present in the **b** direction.

Crystal Structure of 2. Given the extensive modeling necessary for the definition of the correct (albeit approximate) crystal structure of the hydrated form **2**, the intramolecular features within the trinuclear $[Cu_3L(NO_3)_5]^+$ cation will not be discussed. However, the location and orientation of this species in the $P2_1/c$ lattice are reasonably well determined and suggest the following observations:

(a) The coordination environment of Cu1 remains unchanged, i.e., the originally chelating nitrate is still such, although no more lying on a special position. The two sidearms of the complex cation, symmetry related by a 2-fold axis of *C*2/*c* in the anhydrous phase **1**, become different, and the whole moiety is now crystallographically independent.

(b) The (opposite, but coherent) change of the **a** and **c** axes in the **1**-to-**2** transformation requires a slight reorienta-

(38) De Wolff, P. M. *J. Appl. Crystallogr.* **1968**, *1*, 108−113.
(39) Addison, A. W.; Rao, T. N.; Reedijk, J.; Van Rijn, J.; Verschoor, G. C. *J. Chem. Soc., Dalton Trans.* **1984**, 1349−1356.
(40) Eufri, D.; Sironi, A. *J. Mol. Graph.* **1989**, *7*, 165−169.

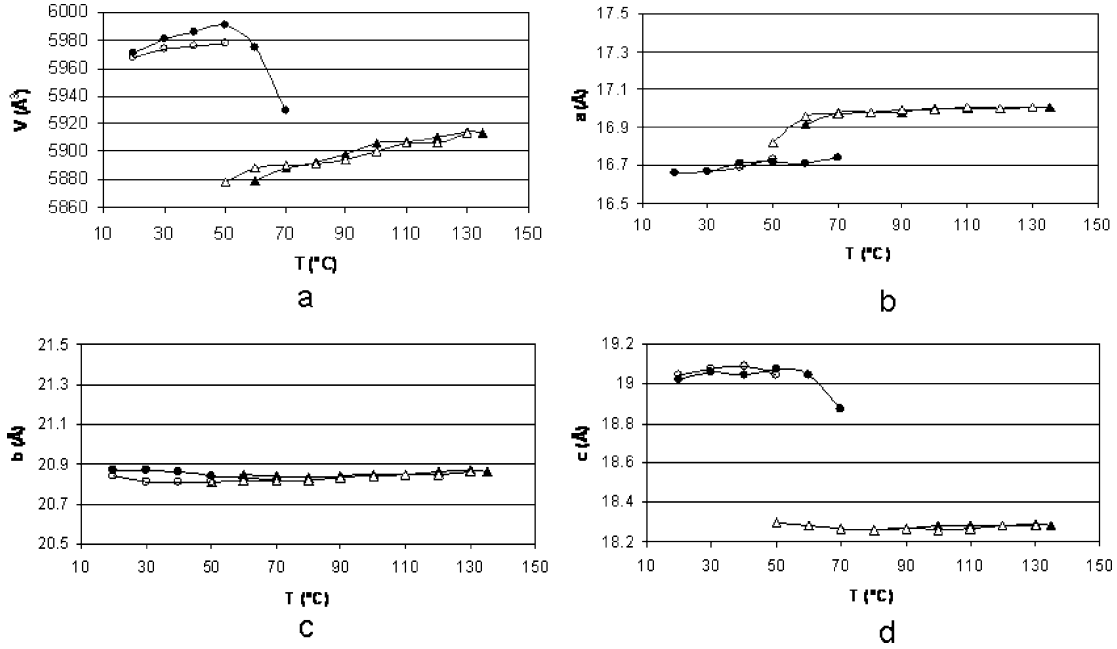

Figure 7. (a) Temperature dependence of the cell volumes of **2** and **1** upon heating (open symbols, 20−135 °C) and subsequent cooling (filled symbols). In (b), (c), and (d), the temperature dependences of the individual axes are plotted.

tion of the molecule, which lengthens the nitrato-bridged Cu···Cu intermolecular interaction from 6.443 up to ca. 7.5 Å.

(c) The pentacoordinated copper atoms adopt a nearly square-planar geometry (as evidenced by the color change upon transformation) with loss of the 'apical' Cu···ONO_2 interactions.

(d) A few holes are generated in the lattice, which host the clathrated water molecules (Figure 1).

Summarizing, a truly ionic species, $[Cu_3L(NO_3)_5](NO_3)$, hosting H_2O molecules is formed upon water addition to crystals of **1**; within the lattice, the formerly bridging nitrate fragment [which showed two 2.378(2) Å contacts with the Cu^{II} ions] is now displaced and shows a much longer Cu···O interaction, approaching 2.60 Å. The driving force in this transformation is not yet clear because no evident stabilizing interactions (e.g., hydrogen bonds) could be assigned to water molecules in species **2**; however, one can tentatively attribute the low stability of **1** to a strained situation, where the bridging nitrate likely pulls together stiff moieties which, in **2**, can relax to a more suitable packing environment, which leaves holes easily filled by water molecules.

Thermodiffractometry. The thermally induced dehydration of **2** was followed by XRPD, which allowed us to estimate a number of interesting crystallochemical features. With reference to Figure 7a, where the cell volumes of **2** (and **1**) at different temperatures during heating to 135 °C and subsequent cooling to room temperature are plotted, it can be easily appreciated that phase **2** has a larger volume than **1** (by about 100 Å^3), thanks to the presence of the clathrated water molecules. These molecules are lost by moderate heating at about 60 °C, and can be reversibly reabsorbed within minutes from aerial moisture by cooling to 50 °C. The thermal expansion coefficients $\alpha = \partial \ln V/\partial T$ derived from the XRPD data are $\alpha = 12.0 \times 10^{-5}$ and 8.9×10^{-5} K^{-1}, for **2** and **1**, respectively, and manifest the rather soft packing forces within the crystals. More importantly, if the temperature dependence of the individual axes are plotted (Figure 7b, c, and d), a different behavior for each of the three can be observed: the variability of the **c** axis (in the 18.28−19.07 Å range) well explains the structural change *induced by cooling*, i.e., the water sorption with the progressive lengthening of the NO_3^- bridged Cu···Cu interaction and the loss of the 'apical' Cu−O interaction (as described above). At variance, the **b** axis is virtually unchanged, by neither temperature nor the occurrence of the water addition/removal process (20.82−20.87 Å), thus confirming the location of the H_2O molecules, which occupy lattice holes within (slightly reoriented) symmetry-related trinuclear complexes sharing the same packing features along **b** (Figure 5). That reorientation about **b** is the physical process occurring during (de)hydration and is also manifested by the temperature dependence of **a**, paralleling that of **c** (even if with the opposite sign).

Once formed, species **1** is stable up to about 250 °C (TG and DSC evidence), without loss of crystallinity. At about 300 °C, about 43% of the initial weight of **1** is lost and a plateau in the TG trace is observed; we tentatively assign to this phase, likely containing partially decomposed ligands, a $Cu_3(NO_3)_6(Lx)$ formulation (M_w ca. 840 g mol^{-1}), with Lx = a heterocyclic ligand derived by loss of eight C_5H_5N units (most likely as dipyridylamine).

Magnetic properties of 2. The temperature dependence of the magnetic susceptibility per trinuclear unit ($\chi_M T$) of **2** was investigated over the temperature range 5−300 K. At room temperature, $\chi_M T$ is equal to 1.10 emu K mol^{-1}, a value compatible with that expected for three independent Cu^{II} ions. As the temperature is lowered, the $\chi_M T$ product slightly increases and reaches a value of 1.25 emu K mol^{-1} at 15 K. This feature indicates very weak intramolecular ferromag-

netic interactions, consistent with the large Cu···Cu separations in the trinuclear unit. Below 15 K, $\chi_M T$ decreases, likely due to antiferromagnetic interactions between the trinuclear units. Given the large magnetic center separations, attempts to fit the magnetic data were not made.

EPR spectra were obtained for polycrystalline sample of **2** at room and liquid nitrogen temperatures. At room temperature, the spectrum shows an absorption at $g_{\|} = 2.19$ with an unresolved broad $g_{\perp}$ signal at 2.10. At low temperature, the spectrum is slightly better resolved. It displays an axially symmetric signal ($g_{\|} = 2.21$, $g_{\perp} \approx 2.12$) assigned to the square planar Cu^{II} ions. A shoulder of the $g_{\perp}$ signal appears at smaller g value ($g \approx 2.09$), likely corresponding to an isotropic absorption, attributed to the Cu^{II} center in the octahedral coordination environment. However, as hyperfine splittings remain unresolved, as a result of exchange narrowing due to the fact that the Cu^{II} ions are too close together, no structural conclusions can be drawn from this method.

Conclusions

In this study, we have explored a solvothermal synthetic procedure to prepare a material which behaves as a moisture-triggered molecular switch. The X-ray single-crystal structure of the polymeric anhydrous phase $[Cu_3L(NO_3)_6]_n$ has been described. The structure of the hydrated phase was retrieved by thorough ab initio X-ray powder diffraction analysis: it is formulated as $[Cu_3L(NO_3)_5](NO_3)\cdot H_2O$ and consists of a $[Cu_3L(NO_3)_5](NO_3)$ ionic species which accommodates one water molecule per newly formed cavity. This contribution thus highlights the high potential of XRPD to solve intricate solid-state structures of supramolecular frameworks presenting tiny structural modifications. Thermodiffraction measurements have revealed that the reported solid-to-solid transformation is fully reversible. Magnetic measurements carried out on the hydrated form have evidenced weak ferromagnetic interactions between the copper centers within the trinuclear unit.

Acknowledgment. This work has been supported financially by the Graduate Research School Combination "Catalysis", a joint activity of the graduate research schools NIOK, HRSMC, and PTN. The Fondazione Provinciale Comasca and the University of Insubria (Progetto di Ateneo "Sistemi Poliazotati") are acknowledged for funding.

Supporting Information Available: X-ray crystallographic data for species **1** and **2** (CIF format); Le Bail plot for **2**. This material is available free of charge via the Internet at http://pubs.acs.org.

IC0509231